On the Validity of the Field Synergy Principle in Elliptic Flows

R. HIMO[a,b], C. HABCHI[b]

a. University of Nantes, Laboratoire de Thermique et Energie de Nantes (LTeN) UMR CNRS6607, B.P. 50609, 1 rue Christian Pauc, 44306 Nantes Cedex 3, France. email : rawad.himo@univ-nantes.fr)
b. Notre Dame University - Louaize, Thermofluids Research Group, P.O. Box : 72 Zouk Mikael, Zouk Mosbeh, Lebanon. email : charbel.habchi@ndu.edu.lb

Abstract :

Local analysis and visualization of convective heat transfer is fundamental for many engineering applications. In fact, the correlation between the flow structure and the transport of heat by advection and diffusion is crucial for designing and optimizing devices undergoing heat transfer, such as heat exchangers. The field synergy principle has been used for more than two decades in order to analyze and enhance the convective heat transfer in different applications. In this paper, the validity of the field synergy principle in elliptic flows is tested for both laminar and turbulent flow regimes. For this end, the flow past a backward facing step is considered for a wide range of Reynolds numbers based on the step height ranging from 36 to 36,000. It is shown that the synergy angle and synergy number both fail to represent the local physics of heat transfer process near the step. This is caused by the assumption of negligible molecular and turbulent thermal diffusivities in this principle. In this paper, it is shown that these diffusivities play a crucial role in heat transfer in elliptic flows and cannot be ignored. Moreover, a global analysis shows that the field synergy number could be used to predict the Nusselt number variation if the elliptic region in the flow is small however, the synergy angle fails here also to characterize the variation in Nusselt number.

Mots clefs : Convective heat transfer, advection transport, diffusion transport, backward facing step, elliptic flows

1 Introduction

Convective heat transfer is found in natural phenomena or in man-made devices and it is thus essential to different fields in physics and engineering. The domain of applications spans over a wide range from simple domestic equipment, industrial devices to weather prediction [1, 2].

Convective heat transfer is the resultant of advective and diffusive transport in a fluid flow. Therefore, it is crucial to understand and characterize locally the effect of the flow structure on the heat transfer phenomena occurring in a given application. This could be done for instance by using the famous “Heatlines" introduced by Kimura and Bejan [3] and based on superposing the heat conduction lines and enthalpy flow lines for a given fluid flow [4]. Other visualization techniques exist in the open literature aiming

to analyze the local flow and heat transfer physics such as the energy streamlines and energy flux vectors [5], field synergy principle [6, 7, 8] and the Lagrangian description [9]. The readers can refer to Mahapatra *et al.* [10] for a review on these different methods.

In this paper, we focus on the validity Field Synergy Principle introduced by Guo *et al.* [6] which is based on modifying the intersection angle between velocity vector and temperature gradient and its application to heat transfer enhancement. This principle has been widely used in the last two decades to study the heat transfer enhancement in parabolic and elliptic flows [11, 12, 13, 14, 15, 16, 17, 18], in which most engineering applications involve elliptic flows. However, the use and validity of this principle has been the issue of much debate, especially when applied to elliptic flows [19, 20, 21, 22, 23]. Hereafter, a brief introduction to the Field Synergy Principle is given.

In 1998, Guo *et al.* [6] published an article based on the analogy between conduction and convection heat transfer in the presence of a heat source. After, integrating the energy equation for a parabolic boundary layer flow, they obtained the following relation between the field synergy number $F_c = Nu_x/\left(Re_x Pr\right)$, introduced later by Guo *et al.* [24], and the dot product of the velocity vector and temperature gradient $\mathbf{u} \cdot \nabla T$:

$$F_c = \frac{\int_0^{\delta_t} \mathbf{u} \cdot \nabla T dy}{U_\infty \left(T_\infty - T_w\right)} \tag{1}$$

Or in other terms :

$$F_c = \frac{\int_0^{\delta_t} |\mathbf{u}| \, |\nabla T| \, cos\left(\beta\right) dy}{U_\infty \left(T_\infty - T_w\right)} \tag{2}$$

It is worthy to note that the field synergy number F_c is similar to the Stanton number widely used to quantify heat transfer problems [22, 23].

According to this relation, Guo *et al.* [6] suggested three ways to enhance the heat transfer process : by increasing the Reynolds and/or Prandlt numbers, increasing the magnitude of the dot product and by increasing the synergy angle β between the velocity vector and the temperature gradient given in Eq. 2. While the first two statements are evident, the third one lacks some accuracy. In fact, and according to Eq. 1 and Eq. 2, the intersection angle between the velocity vector and the temperature gradient β should be far from $n\pi/2$, with n an odd number, and closer to $\left(n-1\right)\pi/2$ in order to enhance the heat transfer process.

A subsequent study by Tao *et al.* [25] suggests the extrapolation of this principle to elliptic flows to cater for most heat transfer problems in engineering. In this study, Tao *et al.* [25] proposed integrating the energy equation in the longitudinal and transverse directions while neglecting the streamwise diffusive term in the fluid $k\partial^2 T/\partial x^2$. Following this method, only global parameters are obtained without gaining insight into the local physics of the heat transfer process. Moreover, we show in the present paper that the effect of streamwise diffusion in the fluid on the heat transfer process is significant for local analysis and thus it cannot be neglected.

Wu and Tao *et al.* [26] later performed a similar study on the flow and heat transfer downstream three-dimensional longitudinal vortex generators where no further improvement is provided on the local variation of the advective transport neither on the local variation of the synergy angle.

As a summary, the field synergy angle, which is the essence of the field synergy principle, can never be used alone to describe the heat transfer process. In this paper we present a detailed and substantial discussion of the validity of the field synergy principle by taking into consideration the effect of the fluid diffusion term in the energy equation, which has been neglected in previous works. Moreover, we perform a local analysis of the different physical parameters participating in the heat transfer phenomena to show that the field synergy principle fails to describe the local physics of convective heat transfer. For this end, numerical simulations are performed for a flow past a backward facing step. The results are first validated against experimental data then the analysis is performed for a wide range of Reynolds numbers from laminar to turbulent flow regimes. The eddy diffusion is also taken into consideration for the turbulent flow and we show that its effect is significant on the field synergy principle.

The paper is organized as follows, in Section 2 we define the computational domain and numerical method adopted, the local analysis of the field synergy principle is given in Setion 3.1 for laminar flow regime and in Section 3.2 for turbulent flow. The global analysis of the Nusselt number and field synergy parameters are given in Section 3.3. Section 4 is devoted for the concluding remarks.

2 Problem Description

2.1 Computational domain and boundary conditions

The computational domain is based on a benchmark provided by the National Aeronautics and Space Administration (NASA) [27] as shown in Fig. 1 for a flow past a backward facing step. The numerical results will be validated against NASA's numerical results and experimental data obtained by Driver and Seegmiller [28] in a subsequent section 2.3.

As stated in the introduction (Section 1), the axial diffusive term in the fluid region $\left(\partial T^2/\partial^2 x\right)$ was neglected in previous studies [6, 25]. To consistently test the validity of the field synergy principle and the assumption that the diffusive transport in the flow direction is insignificant in elliptic flows, the wall heat flux must only emanate vertically in y direction (keeping in mind that heat flux is normal to the boundary). Consequently, all horizontal walls are set to a constant temperature $T_w = 350$ K whereas the only vertical wall, namely the backward facing step, is thermally insulated.

The working fluid is air entering with a uniform velocity profile at constant temperature $T_{in} = 300$ K. Atmospheric pressure is prescribed at the domain outlet. No-slip boundary condition is prescribed on all solid surfaces.

The flow Reynolds number is based on the step height $H = 1$ m and simulations are performed for Reynolds numbers $Re_H = 36$, $Re_H = 360$, $Re_H = 3,600$ and $Re_H = 36,000$; the lowest Reynolds number $Re_H = 36$ exhibits laminar flow, while the highest Reynolds numbers are turbulent.

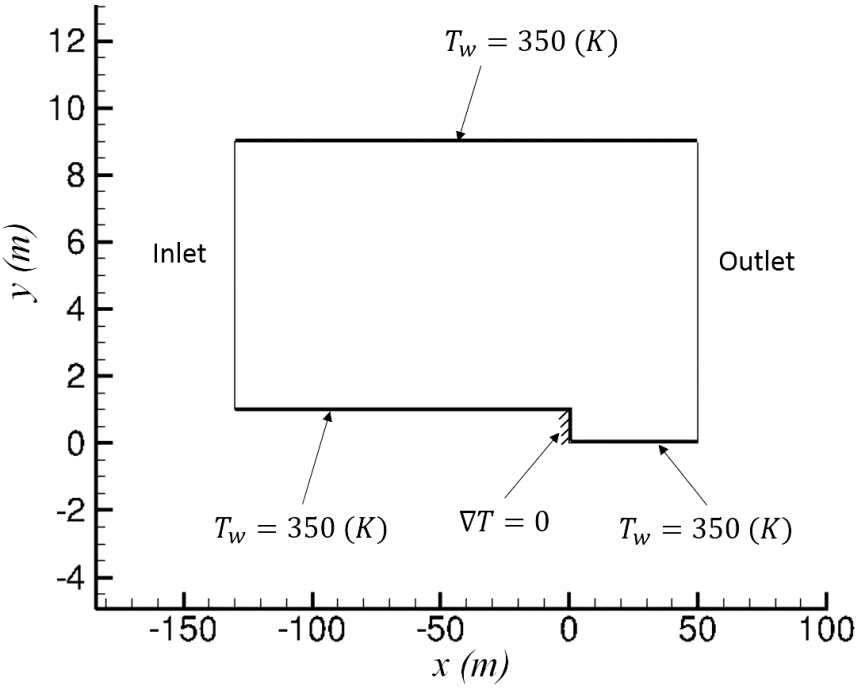

FIGURE 1 – Schematic of the computational domain and boundary conditions (adapted from NASA benchmark [27])

2.2 Governing equations and numerical procedure

The laminar flow field is governed by the two-dimensional (2D) Navier-Stokes equations. The continuity and momentum equations for an incompressible Newtonian fluid are as follows :

$$\nabla \cdot \mathbf{u} = 0 \tag{3}$$

$$\mathbf{u} \cdot \nabla \mathbf{u} = -\frac{1}{\rho}\nabla p + \frac{1}{\rho}\nabla \cdot \mathbb{S} \tag{4}$$

In the linear momentum equation $\mathbb{S}$ is the viscous stress tensor :

$$\mathbb{S} = \mu \left[\nabla \mathbf{u} + \nabla \mathbf{u}^T\right] \tag{5}$$

The energy equation is given by :

$$\rho c_p \nabla \cdot (\mathbf{u}T) = k_f \nabla^2 T \tag{6}$$

where c_p is the specific heat and k_f is the molecular thermal conductivity.

The turbulent flow is modeled by the two-dimensional (2D) Reynolds Averaged Navier-Stokes (RANS) equations. While the continuity equation remains unchanged, the momentum equation for turbulent incompressible Newtonian fluid flows becomes as follows :

$$\mathbf{u} \cdot \nabla \mathbf{u} = -\frac{1}{\rho}\nabla p + \frac{1}{\rho}\nabla \cdot \mathbb{S} - \mathbf{u}'\nabla \mathbf{u}' \tag{7}$$

The term $\mathbf{u}'\nabla\mathbf{u}'$ is the Reynolds stress tensor resulting from the averaging procedure on the nonlinear convective terms in the momentum equations. This term is computed by the Prandtl closure hypothesis with the $k-\omega$ SST (Shear Stress Transport) turbulence model [29].

The energy equation is also computed in the fluid domain and is given by :

$$\rho c_p \nabla \cdot (\mathbf{u}T) = \nabla \cdot (k_{eff}\nabla T) \tag{8}$$

where $k_{eff} = k_f + k_t$ to account for the effect of turbulent fluctuations as modeled by the turbulent Prandtl analogy embedded in $k-\omega$ SST model.

The solver used for the flow computation is the CFD code ANSYS Fluent 18.0 [30], which is based on cell-centered finite volume discretization method. The governing equations are solved sequentially with double precision and a second-order upwind scheme [31] for spatial discretization of the convective terms. The diffusion terms are central differenced and second-order accurate. Pressure-velocity coupling is achieved by the SIMPLE algorithm [30].The residual value 10^{-6} is set as the convergence criterion for the solutions of the flow and energy equations. Beyond this value no significant changes were observed in the velocity and temperature fields.

2.3 Meshing and experimental validation

A non-uniform structured two-dimensional mesh is generated while paying special attention to the near-wall refinement at all solid boundaries and near the backward facing step, so as to take into account the high velocity and temperature gradients in these regions.

The different mesh densities and their main features are given in Table 1. To determine the appropriate mesh density for solution grid independence, the solver is run with increasing mesh densities until no significant effect on the results is detected. The mesh validity verification is performed by using the method proposed by Celik [32] where the grid convergence index (GCI) and the apparent order of convergence p_c can be obtained. The mesh validity verification is applied to the global Nusselt number Nu (Eq.(9)) representing the ratio of convective to conductive heat transfer :

$$Nu = \frac{hH}{k_f} \tag{9}$$

where h is the overall convective heat transfer coefficient $(\mathrm{W/m^2K})$, $H(\mathrm{m})$ the step height and $k_f(\mathrm{W/mK})$ is the thermal conductivity of the working fluid.

In Eq.(10), h is calculated from the logarithmic mean temperature difference :

$$h = \frac{\dot{q}}{A\Delta T_{lm}} \tag{10}$$

where $\dot{q}$ is the overall rate of heat transfer (W) defined in Eq.(11), A $(\mathrm{m^2})$ is the heat transfer area and ΔT_{lm} is the logarithmic mean temperature difference defined in Eq.(12).

$$\dot{q} = \dot{m} c_p \Delta T \tag{11}$$

where $\dot{m}$ is the mass flow rate (kg/s) and $\Delta T = T_{out} - T_{in}$ is the bulk temperature difference between the inlet and outlet.

$$\Delta T_{lm} = \frac{(T_w - T_{in}) - (T_w - T_{out})}{ln(\frac{T_w - T_{in}}{T_w - T_{out}})} \tag{12}$$

As shown in Table 1, the uncertainty in the fine-grid solution is found to be about 0.02% and the order of convergence is 7.6. Therefore, the last mesh is considered for all simulations. For more details about the calculation of the parameter GCI and p_c, the readers can refer to Celik [32]. It should be noted that the mesh study presented here is performed for the highest Reynolds number *i.e.* $Re_H = 36,000$ representing the critical case due to highest fluctuations and gradients. The fine mesh is then used for the lower Reynolds numbers insuring good accuracy of the numerical results.

The numerical simulations are performed on eight parallel Intel® Core™ i7-7700 2.80 GHz processors. Each run takes around one day to converge.

TABLE 1 – Mesh characteristics and sensitivity analysis

Cell number n	224,556	402,864	1,268,245
Mesh size $l = (V/n)^{1/2}$ (mm)	0.0815	0.061	0.034
Global Nusselt number Nu	58.47	58.47	59.15
Grid Convergence Index $GCI(\%)$	–	–	0.02
Apparent order of convergence p_c	–	–	7.60

The numerical method is validated with experimental data obtained by Driver and Seegmiller [28] using Laser Dopler Velocimetry and with numerical data reported by NASA [27] using SST turbulence model [29] for a Reynolds number of 36,000. The axial velocity profiles at several x/H positions from the actual study are compared to those obtained from experimental and numerical simulations as shown in Fig. 2. From this figure, it could be concluded that a fair agreement is obtained between actual CFD results and those obtained in the literature. The maximum relative error did not exceed 4% between the present study and NASA's numerical results. In this figure, U_{ref} is the reference velocity at the center-channel near $x/H = -4$ used to normalize the velocity.

3 Results and Discussion

In this section, the Nusselt numbers are calculated using three different methods. To avoid redundancy and confusion, we denote :

• Nu^q the Nusselt number calculated based on the wall heat flux obtained directly from the CFD results on the solid boundaries.

• Nu^s the Nusselt number calculated based on the Field Synergy principle from Eq.(13).

• Nu^c the Nusselt number calculated based on the corrected formulae from Eq.(16) for laminar flows and Eq.(22) for turbulent flows.

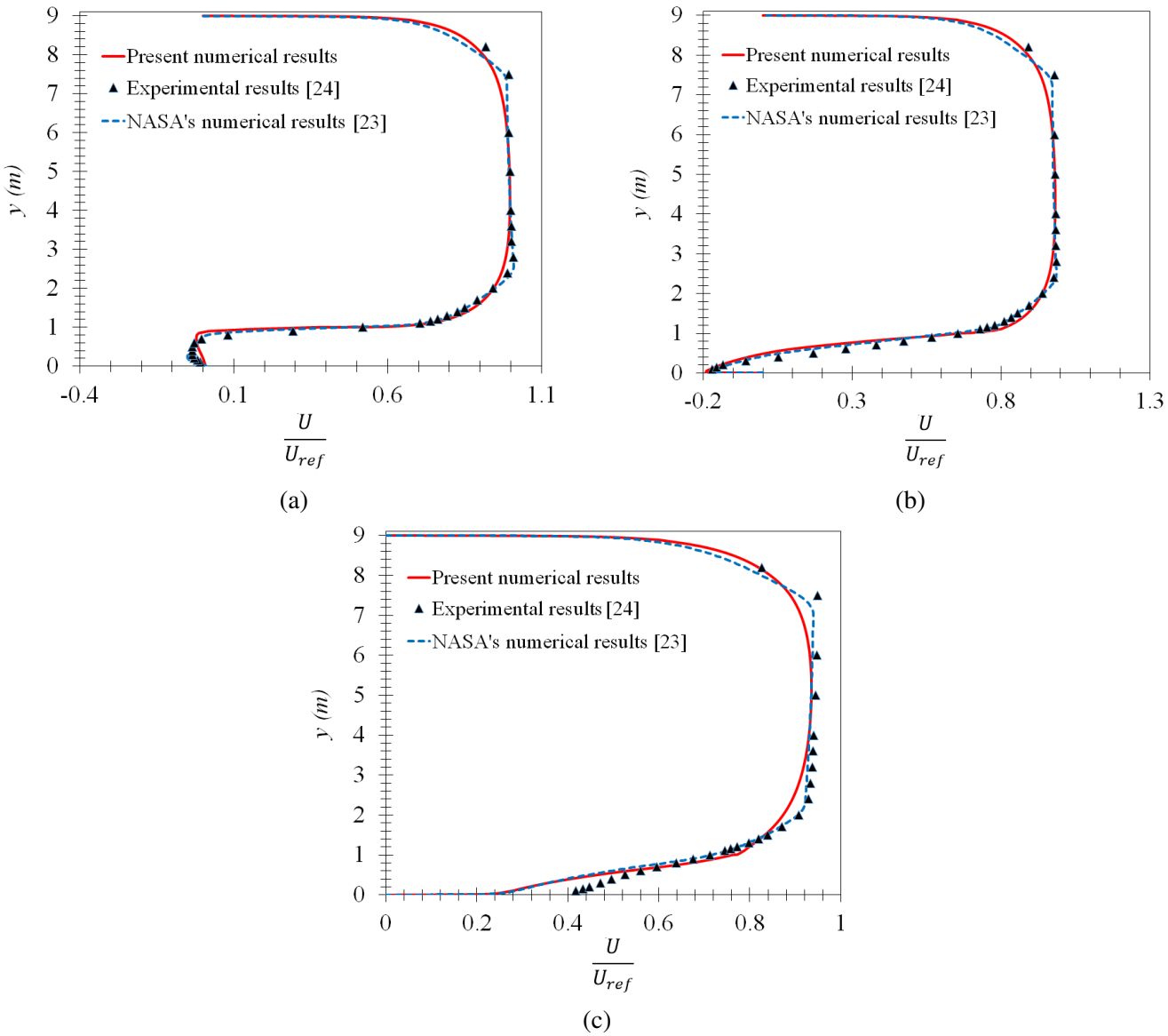

FIGURE 2 – Axial velocity profiles at $x = 1$ (a), $x = 4$(b) and $x = 10$ (c)

3.1 Laminar flow

Starting from the following Eq.(13) which is the y integration of the energy equation for a laminar parabolic flow :

$$\rho c_p \int_0^{\delta_{th}} \left(u\frac{\partial T}{\partial x} + v\frac{\partial T}{\partial y} \right) dy = -k_f \frac{\partial T}{\partial y}\bigg|_w \tag{13}$$

Eq.13 could also be written as follow :

$$\rho c_p \int_0^{\delta_{th}} \left(|\mathbf{u}| \cdot |\nabla T| \cdot cos\left(\beta\right) \right) dy = q_w \tag{14}$$

Guo's "Novel concept for convective heat transfer" suggested three possible ways to increase the heat transfer and they are :

• Increasing the Reynolds and Prandlt numbers

• Increasing the fullness of dimensionless velocity and temperature profiles which he defined as $\overline{U} = \frac{U}{U_\infty}$ and $\nabla\overline{T} = \frac{\nabla T}{(T_\infty - T_w)/\delta_{th}}$

• Increasing the angle between the velocity and temperature gradient vectors. (Later published by Tao [25] as the decrease in the angle which will cause the increase in $cos(\beta)$)

While the first two suggestions are self evident, the last one presents an obvious overlooking of the fact that the simplified version of the energy equation becomes obsolete when the synergy angle is changed, since the diffusive transport in the axial direction can no longer be neglected due to the fact that the whole flow structure has changed locally.

A more correct representation of the heat transfer in an elliptic flow should be as follows. Starting from the complete energy equation in a two dimensional flow :

$$\rho c_p \left(u\frac{\partial T}{\partial x} + v\frac{\partial T}{\partial y} \right) = \frac{\partial}{\partial x}\left(k_f \frac{\partial T}{\partial x} \right) + \frac{\partial}{\partial y}\left(k_f \frac{\partial T}{\partial y} \right) \tag{15}$$

Isolating and integrating in the y direction :

$$q_w = k_f \frac{\partial T}{\partial y}\bigg|_w = \rho c_p \int_0^{\delta_{th}} \left(u\frac{\partial T}{\partial x} + v\frac{\partial T}{\partial y} \right) dy - \int_0^{\delta_{th}} \frac{\partial}{\partial x}\left(k_f \frac{\partial T}{\partial x} \right) dy \tag{16}$$

or,

$$q_w = k_f \frac{\partial T}{\partial y}\bigg|_w = \rho c_p \int_0^{\delta_{th}} \left(|\mathbf{u}| \cdot |\nabla T| \cdot cos\left(\beta\right) \right) dy - \int_0^{\delta_{th}} \frac{\partial}{\partial x}\left(k_f \frac{\partial T}{\partial x} \right) dy \tag{17}$$

Eq. 17 shows that the heat flux, i.e. the Nusselt number, depends on both : advection and diffusion. The advection term was described by Tao *et al.* [25] as the Synergy, and the diffusion is totally neglected. Now we will show how that the field synergy principle and the synergy angle β are not representative of the local heat transfer in elliptic flows.

Calculating the local Nusselt number based on the step height H from q_w according to Eq. (18), the validity of the field synergy principle can be put to the test.

$$Nu_x = \frac{q_w H}{k_f \left(T_w - T_b\right)} \tag{18}$$

where T_b is the fluid bulk temperature at given x/H.

The results of the local Nusselt are shown in Fig. 3 from the wall heat flux obtained from CFD results (as Nu_x^q in red), from synergy in Eq.13 (as Nu_x^s in black) and from the present study's modified equation in Eq.16 (as Nu_x^c in blue).

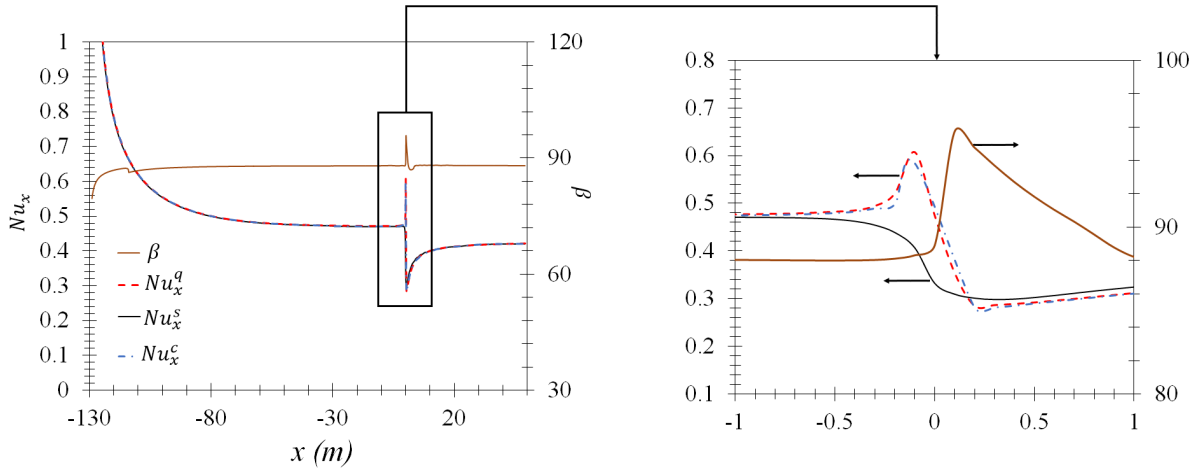

FIGURE 3 – Local Nusselt number from the different methods along with local the synergy angle

From this figure, it could be observed that the Field Synergy principle's assumption is valid throughout the entrance and the developed region of the flow, except near the proximity of the step. That's where the synergy angle is varied greatly, hence the claim that the convective heat transfer can be improved by increasing the synergy angle becomes unreliable since the equation defining this principle is not fully representative of the heat transfer. A close-up on the variation of the Nusselt numbers near the step is shown also in Fig. 3 to the right side, where it is clear that the behavior of the transport described in Eq.13 (using the Field Synergy principle) is completely different than the actual phenomenon. However, the present study's claim of the importance of the diffusive transport in the streamwise direction upon the change in the flow structure is clearly representing the transfer of the thermal energy.

In addition, from Fig. 3, one can evaluate the claim that the increase in the synergy angle is a way to increase the heat transfer is misleading, once the Nusselt number is juxtaposed with the synergy angle. In fact, an opposite behavior is witnessed after $x = 0$ where the increased in β is mirrored by a decrease in Nu_x^q and vice versa. The reason behind this discrepancy can be simply explained by referring to the energy equation (Eq.6) where the dot product of the advective term can be rewritten as the multiplication of both magnitudes of $\mathbf{u}$ and ∇T with the cosine of the synergy angle. Consequently, it is more fair to analyze the heat transfer vis-à-vis the variation in $cos(\beta)$ as shown in Fig. 4.

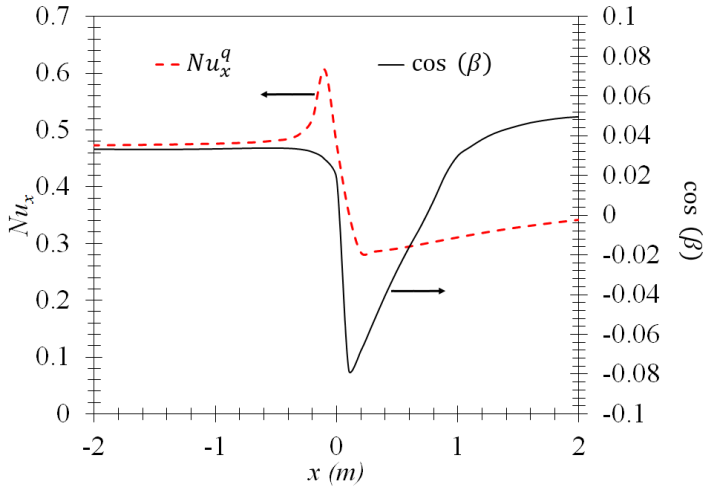

FIGURE 4 – A close up on the Local Nusselt number for the different methods and $cos(\theta)$

Obviously, $cos(\beta)$ in the advective term is not solely responsible for the heat transfer since it did not reflect the increase in the local Nusselt number at $x < 0$, due to the presence of the prominent diffusive term especially when the synergy angle is changing, which further supports the claim in this manuscript. This issue will be further elaborated by showing the contribution of each of the advective and diffusive terms given by the following equations respectively and shown in Fig. 5.

$$\psi = \rho c_p \int_0^{\delta_{th}} \left(u \frac{\partial T}{\partial x} + v \frac{\partial T}{\partial y} \right) dy \tag{19}$$

$$\xi = \int_0^{\delta_{th}} \frac{\partial}{\partial x} \left(k_f \frac{\partial T}{\partial x} \right) dy \tag{20}$$

The results in Fig. 5 further support the claim that diffusion cannot be neglected in elliptic laminar flows especially near the step where the flow will be modified. Hence, the effect of the diffusion term is responsible for the increase in the local Nusselt number near the step as shown in Fig. 4.

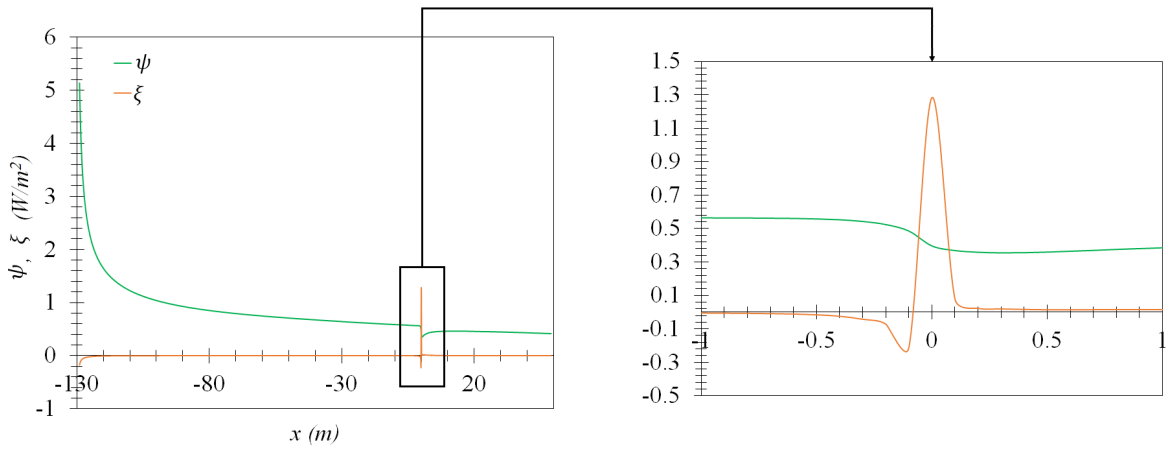

FIGURE 5 – Variation of ψ and ξ terms with X

3.2 Turbulent flow

In this section we will consider turbulent flow regime. The energy equation computed by $k-\omega\ SST$ including the turbulent prandtl analogy is as follows :

$$\rho c_p\left(u\frac{\partial T}{\partial x}+v\frac{\partial T}{\partial y}\right)=\frac{\partial}{\partial x}\left(k_f\frac{\partial T}{\partial x}\right)+\frac{\partial}{\partial y}\left(k_f\frac{\partial T}{\partial y}\right)+\frac{\partial}{\partial x}\left(k_t\frac{\partial T}{\partial x}\right)+\frac{\partial}{\partial y}\left(k_t\frac{\partial T}{\partial y}\right) \tag{21}$$

where k_t is the turbulent eddy conductivity.

Isolating and integrating in the y direction :

$$q_w=k_f\frac{\partial T}{\partial y}=\rho c_p\int_0^{\delta_{th}}\left(u\frac{\partial T}{\partial x}+v\frac{\partial T}{\partial y}\right)dy-\int_0^{\delta_{th}}\frac{\partial}{\partial x}\left(k_f\frac{\partial T}{\partial x}\right)dy-\int_0^{\delta_{th}}\left[\frac{\partial}{\partial x}\left(k_t\frac{\partial T}{\partial x}\right)+\frac{\partial}{\partial y}\left(k_t\frac{\partial T}{\partial y}\right)\right]dy \tag{22}$$

When the local Nusselt number based on the step height H is calculated from q_w, the validity of the Field Synergy principle for elliptic turbulent flows can be put to the test. The results of the local Nusselt are shown in Fig. 6 from the wall heat flux, from Eq.13 and from the present study's claim in Eq.22.

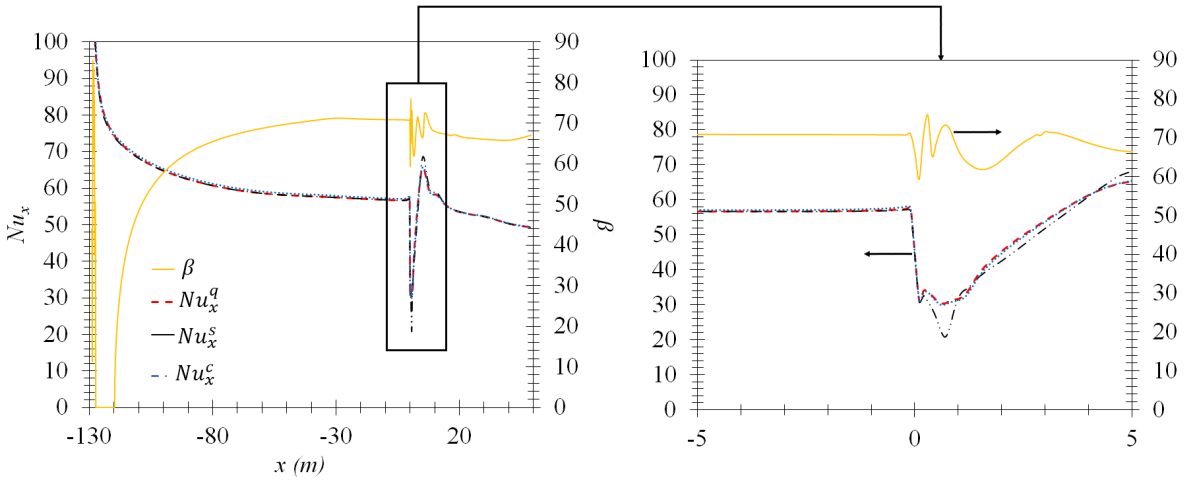

FIGURE 6 – Local Nusselt number for the different methods and the synergy angle for $Re=36,000$

Similar to the laminar case, the claim of the Field Synergy principle is compromised near the step, where the synergy angle is varied greatly as shown in Fig. 6. On the other hand, when the full energy equation is taken into account such as in Eq.22 the heat transfer is described with good accuracy. This means that the diffusive and turbulent transports of the thermal energy are contributing to the heat transfer and could not be neglected as assumed by Tao *et al.* [25] in elliptic flows.

The contribution of each of the advective ψ, diffusive ξ and turbulent transport ξ_t, given in Eq. (23), are shown in Fig. 7. This figure highlights the importance of diffusive and turbulent transport terms relative to the advective term. Thus neglecting these terms induces variance between the computed Nusselt number and that obtained using the field synergy principle.

$$\xi_t=\int_0^{\delta_{th}}\left[\frac{\partial}{\partial x}\left(k_t\frac{\partial T}{\partial x}\right)+\frac{\partial}{\partial y}\left(k_t\frac{\partial T}{\partial y}\right)\right]dy \tag{23}$$

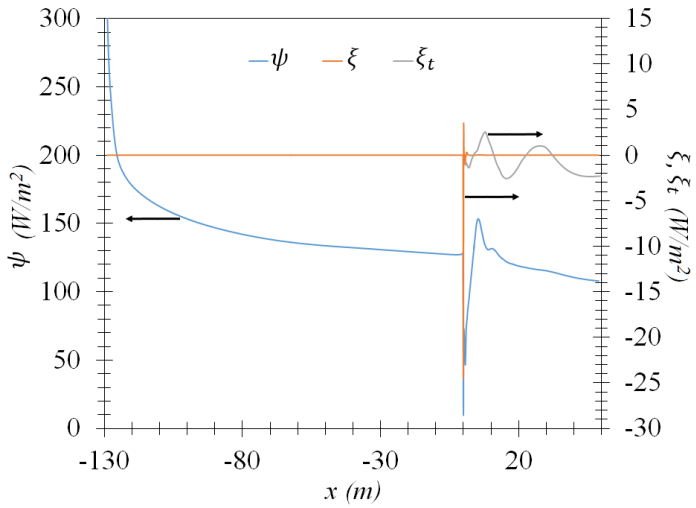

FIGURE 7 – Variation of ψ, ξ and ξ_t terms with x

The ratio of the Nusselt number derived from the synergy (Nu_x^s) over the actual span-averaged local Nusselt number obtained from CFD or full energy equation (Nu_x^q) is shown in Fig. 8. It could be observed that near the step, where the flow is classified as elliptic flow, the field synergy principle induces a relative error of about 32%, even in a highly turbulent case with a high Péclet number, in opposition to the claim of Tao *et al.* [25] who claimed that the field synergy principle works well for high Péclet numbers.

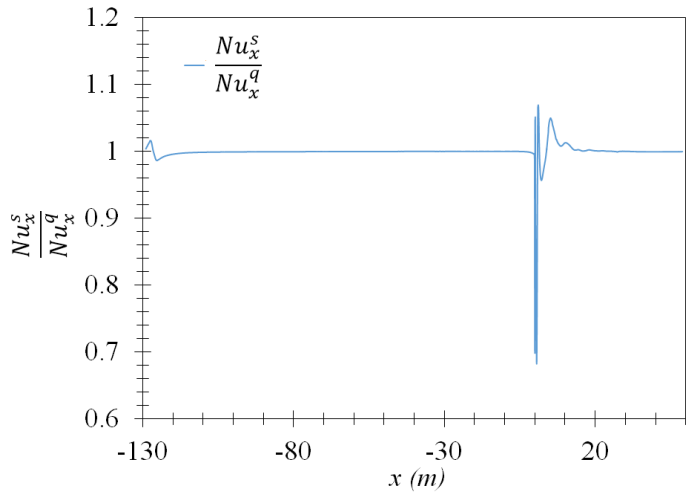

FIGURE 8 – Variation of $\frac{Nu_x^s}{Nu_x^q}$ with x

3.3 Global analysis

In this section of this manuscript, the global Nusslet number and synergy angle variation with Reynolds number is analyzed as shown in Fig. 9. As shown in this figure, the Nusselt number increases with increasing Reynolds number while $cos(\beta)$ varies slightly between 0.048 and 0.056 and shows a maximum at a Reynolds of 3,600. Beyond this Reynolds number $cos(\beta)$ decreases opposing to the variation in Nusselt number. Thus it could be concluded that $cos(\beta)$ cannot be used alone to represent the global heat transfer as for the local analysis.

In addition, the Stanton number, sometimes referred to as the Field synergy number, shows a decreasing behavior with increasing Reynolds number, due to the increase of Re at a higher rate than the increase of the global Nusselt number.

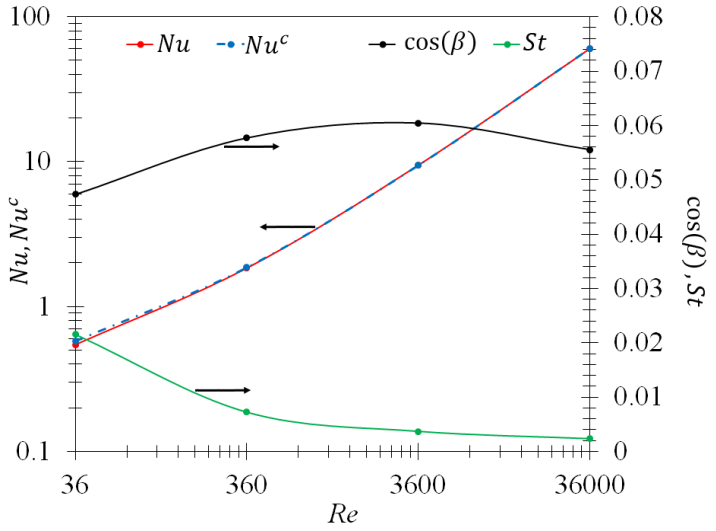

FIGURE 9 – Global Nu and cosine of the average Synergy angle vs. Re_H

4 Conclusion

Field synergy principle was extensively used to study parabolic and elliptic convective heat transfer. In this paper we study the validity of this principle by considering the flow past a backward facing step for both laminar and turbulent flow regimes.

The concluding remarks are summarized as follows :

• The assumption that the molecular thermal diffusivity in the streamwise direction is negligible proves to be invalid for elliptic flows. Therefore, the field synergy number and synergy angle cannot be used to describe the local heat transfer process.

• In turbulent flow regimes, neglecting the turbulent thermal diffusivity led to misleading results in the field synergy parameters and thus this principle fails to describe accurately the physics of heat transfer near the step.

• If the elliptic region in the flow is small relative to the overall computational domain, the field synergy number can be used to predict the variation in the overall Nusslet number. However, special care should be taken into consideration when dealing with complex geometries in which elliptic regions are dominant.

• The field synergy angle cannot be used alone to describe local and global variation in the Nusselt number or convective heat transfer coefficient.

Références

[1] L. Theodore, Heat Transfer Applications for the Practicing Engineer, 1st Edition, Wiley, 2011.

[2] A. Bejan, Convection Heat Transfer, 4th Edition, Wiley, 2013.

[3] S. Kimura, A. Bejan, The "Heatline" visualization of convective heat transfer, Journal of Heat Transfer, 105 (1983) 916–919.

[4] A. Morega, A. Bejan, Heatline visualization of forced convection laminar boundary layers, International Journal of Heat and Mass Transfer, 36 (1993) 3957–3966.

[5] S. Mahmud, R. Fraser, Visualizing energy flows through energy streamlines and pathlines, International Journal of Heat and Mass Transfer, 50 (2007) 3990–4002.

[6] Z.-Y. Guo, D.-Y. Li, B.-X. Wang, A novel concept for convective heat transfer enhancement, International Journal of Heat and Mass Transfer, 41 (1998) 2221–2225.

[7] Y. Li, Q. Liu, R. Cai, Explicit analytical solutions for fluid flow and temperature
eld synergy in cylindrical coordinates, International Journal of Thermal Sciences, 54 (2012) 119–124.

[8] L. Ma, J. Yang, W. Liu, X. Zhang, Physical quantity synergy analysis and efficiency evaluation criterion of heat transfer enhancement, International Journal of Thermal Sciences, 80 (2014) 23–32.

[9] M. Speetjens, A generalised lagrangian formalism for thermal analysis of laminar convective heat transfer, International Journal of Thermal Sciences, 61 (2012) 79–93.

[10] P. Mahapatra, A. Mukhopadhyay, N. Manna, K. Ghosh, Heatlines and other visualization techniques for confined heat transfer systems, International Journal of Heat and Mass Transfer, 118 (2018) 1069–1079.

[11] J. E, W. Zuo, H. Liu, Q. Peng, Numerical investigation of helically coiled tube from the viewpoint of field synergy principle, Applied Thermal Engineering, 93 (2016) 83–89.

[12] J. Li, H. Peng, X. Ling, Numerical study and experimental verification of transverse direction type serrated fins and field synergy principle analysis, Applied Thermal Engineering, 54 (2013) 328–335.

[13] C.-C. Chang, Y.-T. Yang, T.-H. Yen, C.-K. Chen, Numerical investigation into thermal mixing efficiency in y-shaped channel using lattice boltzmann method and field synergy principle, International Journal of Thermal Sciences, 48 (11) (2009) 2092–2099.

[14] Y. Cheng, T. Lee, H. Low, Numerical simulation of conjugate heat transfer in electronic cooling and analysis based on field synergy principle, Applied Thermal Engineering, 28 (2008) 1826–1833.

[15] J. Guo, X. Huai, Numerical investigation of helically coiled tube from the viewpoint of field synergy principle, Applied Thermal Engineering, 98 (2016) 137-143.

[16] G. Lu, G. Zhou, Numerical simulation on performances of plane and curved winglet pair vortex generators in a rectangular channel and field synergy analysis, International Journal of Thermal Sciences, 109 (2016) 323–333.

[17] Z. Zhu, J. Zhao, Improvement in field synergy principle : More rigorous application, better results, International Journal of Heat and Mass Transfer, 100 (2016) 347–354.

[18] B. Mehra, J. Simo Tala, C. Habchi, J. Harion, Local field synergy analysis of conjugate heat transfer for different plane fin configurations, Applied Thermal Engineering, 130 (2018) 1105–1120.

[19] C. Habchi, T. Lemenand, D. D. Valle, L. Pacheco, O. L. Corre, H. Peerhossaini, Entropy production and field synergy principle in turbulent vortical flows, International Journal of Thermal Sciences, 50 (2011) 2365–2376.

[20] B. Zhang, M. O. Hamid, W. Liu, Applied Thermal Engineering, 99 (2016) 944–958.

[21] A. Bejan, Heatlines (1983) versus synergy (1998), International Journal of Heat and Mass Transfer, 81 (2015) 654–658.

[22] M. Awad, Field synergy number versus Stanton number, Thermal Science, 19 (2015) 739–741.

[23] A. Bejan, Comment on Study on the consistency between fi
eld synergy principle and entransy dissipation extremum principle, International Journal of Heat and Mass Transfer, 120 (2018) 1187–1188.

[24] Z. Guo, W.-Q. Tao, R. Shah, The field synergy (coordination) principle and its applications in enhancing single phase convective heat transfer, International Journal of Heat and Mass Transfer, 48 (2005) 1797–1807.

[25] W.-Q. Tao, Z.-Y. Guo, B.-X. Wang, Field synergy principle for enhancing convective heat transfer its extension and numerical verification, International Journal of Heat and Mass Transfer, 45 (2002) 3849–3856.

[26] J.-M. Wu, W.-Q. Tao, Numerical study on laminar convection heat transfer in a rectangular channel with longitudinal vortex generator. Part a : Verification of field synergy principle, International Journal of Heat and Mass Transfer, 51 (2008) 1179–1191.

[27] C. Rumsey, 2D backward facing step, Technical report, Langly Research Center, National Aeronautics and Space Administration (NASA) (2016). URL https ://turbmodels.larc.nasa.gov/backstep_val.html.

[28] D. M. Driver, H. L. Seegmiller, Features of reattaching turbulent shear layer in divergent channel flow, AIAA Journal 23 (1985) 163–171.

[29] F. Menter, Two-equation eddy-viscosity turbulence models for engineering applications, AIAA Journal 32 (1994) 1598–1605.

[30] ANSYS, Academic Research, Release 18.0.

[31] R. Warming, R. Beam, Upwind second-order difference schemes and applications in aerodynamic flows, AIAA Journal, 14 (1976) 1241–1249.

[32] I. Celik, U. Ghia, P. Roache, H. Freitas, Procedure for estimation and reporting of uncertainty due to discretization in CFD applications, Journal of Fluids Engineering, 130 (2008) 078001.